



A simplified climate model with combined atmospheric-hydrological processes

M. NAKATSUGAWA , M. ANDERSON & M. L. KAWAS

To cite this article: M. NAKATSUGAWA , M. ANDERSON & M. L. KAWAS (1996) A simplified climate model with combined atmospheric-hydrological processes, Hydrological Sciences Journal, 41:6, 915-938, DOI: [10.1080/02626669609491559](https://doi.org/10.1080/02626669609491559)

To link to this article: <http://dx.doi.org/10.1080/02626669609491559>



Published online: 24 Dec 2009.



Submit your article to this journal [↗](#)



Article views: 71



View related articles [↗](#)



Citing articles: 2 View citing articles [↗](#)

A simplified climate model with combined atmospheric-hydrological processes

M. NAKATSUGAWA

*Civil Engineering Research Institute, Hokkaido Development Bureau,
Sapporo 062, Japan,*

M. ANDERSON & M. L. KAVVAS

*Department of Civil and Environmental Engineering, University of California,
Davis, California 95616, USA*

Abstract Global climate change can be reproduced in detail by using three-dimensional general circulation models (GCMs). However, such complex models require super-computers and extensive hours of computational time for a single attempt at reproducing long term climate change. An alternative approach is to make simplifying assumptions that retain the essential physics for the desired simulation. Energy balance and radiative-convective models are examples of such models. The model in this study follows the simplified approach using physics-based climate processes as well as interactions between atmospheric and hydrological processes. The vertically and latitudinally averaged mean temperature and mean water vapour content between 30°N-50°N latitudes are considered as atmospheric state variables while soil and sea temperatures and water storage amount are considered for describing the behaviour of the hydrological system. Temperatures in both the atmosphere and ground are calculated by a thermal energy equation that considers the physically-based processes of shortwave radiation, longwave radiation, sensible heat flux, and latent heat flux. Precipitation and evaporation processes transport moisture between the atmosphere and ground. In this study, the radiation parameterization of the simplified climate model is tested in the investigation of the various effects of global warming due to doubling and quadrupling of CO₂. Changes of temperature, soil water content, evaporation rate and precipitation rate are investigated by numerical experiments. The simplified climate model provides acceptable simulation of climate change and holds promise for practical investigations such as the interactions of physical processes in the evolution of drought phenomena.

Un modèle simplifié du climat combinant les processus atmosphériques et hydrologiques

Résumé Le changement du climat planétaire peut être reproduit en détail en utilisant des modèles tridimensionnels de la circulation générale. Mais des modèles aussi complexes exigent des ordinateurs puissants ainsi que de nombreuses heures de calcul pour ne simuler qu'un seul scénario d'évolution à long terme du climat. Une alternative serait de faire des hypothèses simplificatrices ne retenant que les processus physiques essentiels pour la simulation désirée. Les modèles "bilan d'énergie" et "radiatif-convectif" sont des exemples de tels modèles. Le modèle présenté dans cette étude suit l'approche simplifiée en prenant en compte des processus climatiques fondés sur des phénomènes physiques comprenant des interactions entre des processus atmosphériques et hydrologiques. La température moyenne verticale et latérale et le contenu moyen en vapeur d'eau entre les latitudes

30 et 50°N sont considérés comme des variables d'état de l'atmosphère alors que les températures du sol et de la mer et l'emmagasinement de l'eau sont considérés en vue de décrire le comportement du système hydrologique. Les températures dans l'atmosphère et sur la terre sont calculées grâce à une équation de l'énergie thermique qui prend en compte les phénomènes radiatifs dans la gamme des courtes et grandes longueurs d'onde, le flux de chaleur sensible et le flux de chaleur latente. Les processus de précipitation et d'évaporation transportent l'humidité entre l'atmosphère et le sol. Dans cette étude, nous mettons à l'épreuve la paramétrisation des phénomènes radiatifs du modèle climatique simplifié dans notre étude des différents effets du réchauffement global résultant du doublement ou du quadruplement du CO₂. Les modifications de la température, de l'humidité du sol, de l'évaporation et des précipitations sont testées grâce à des expériences numériques. Le modèle simplifié du climat fournit une simulation acceptable du changement climatique et devrait être utile pour des recherches appliquées comme par exemple celle de l'interaction des processus physiques impliqués dans l'évolution du phénomène de sécheresse.

INTRODUCTION

The climate system is defined as being composed of the atmosphere, hydrosphere, cryosphere, biosphere and land surface. Simplified models that balance the planetary radiation budget offer a first insight into the evolution of the Earth's climate. Budyko (1969) and Sellers (1969, 1973) stimulated interest in models of this type, which are called Energy Balance Models (EBMs). Variation of the surface temperature with latitude is reproduced by one-dimensional EBMs. One-dimensional radiative-convective (RC) models compute the vertical temperature profile by explicitly modelling the radiative processes including a thermal adjustment due to convection. Earlier work involved in RC models has been performed by Manabe & Wetherald (1967), and Ramanathan & Coakley (1979). Saltzman (1978) provided a review of EBMs and RC models of the terrestrial climate. Other work linking dynamic hydrology and climate through thermal and hydrological balances has been accomplished by Eagleson (1970, 1978). It is important to note that the one-dimensional nature of both the EBMs and RC models does not allow for the investigation of the more detailed regional climate change.

General circulation models (GCMs) with a full three-dimensional representation of the atmosphere and ocean are the most complete climate models currently available. Manabe & Bryan (1969) at the NOAA Geophysical Fluid Dynamics Laboratory (GFDL) made the first attempt at modelling the atmosphere, ocean and cryosphere. Since then, many GCMs have been developed for global climate change investigations. GCMs have been developed by GFDL, the Goddard Institute for Space Studies (GISS) (Hansen *et al.*, 1988), the National Center for Atmospheric Research (NCAR) (Washington & Williamson, 1977), the United Kingdom Meteorological Office (UKMO) (Corby *et al.*, 1977) and the Japanese Meteorological Research Institute (MRI, 1984). Simmons & Bengtsson (1988) provided a review of general circulation models and their use in climate studies.

However, large amounts of CPU time and memory are required for the computation of long term climate change by GCMs even when running simulations on super-computers. In order to reduce significantly the computational burden, Bravar & Kavvas (1991) proposed a simplified general circulation model that maintains the physics-based processes of the climate system. In their study, only two atmospheric state variables and two hydrological state variables over a mid-latitude band between 30°N and 50°N are integrated with time during climate simulation. Atmospheric temperature and water vapour content are averaged in the troposphere leaving the west-east direction as the only remaining spatial coordinate.

This paper presents a significantly modified version of the one-dimensional model of Bravar & Kavvas (1991). First, the basic equations of the model are reviewed. The next section of the paper then presents the parameterizations added to the original model, and the results of numerical experiments involving climate change due to increasing CO_2 are given in the final section.

BASIC MODEL EQUATIONS

In the simplified climate model, computational effort is reduced by using Rossby wave components for estimating the longitudinal advection based on quasi-geostrophic theory at mid-latitudes instead of solving the three-dimensional components of atmospheric motions. Climatic mechanisms included in the model are shown schematically in Fig. 1. The governing equations with respect to the four state variables used in the model (atmospheric temperature, atmospheric water content, land/sea surface temperature, and water storage) are described below.

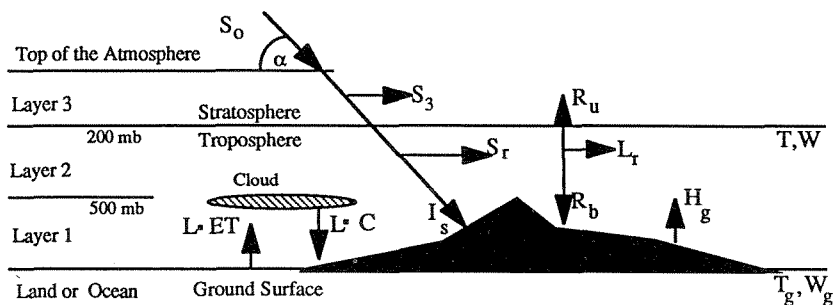


Fig. 1 Schematic illustration of climate system components in the model.

Atmospheric thermal balance

The atmospheric temperature equation is based on the first law of thermodynamics applied to an air parcel as follows:

$$c_p \rho \frac{dT}{dt} = \frac{dp}{dt} + \frac{dq}{dt} \quad (1)$$

where T is the atmospheric temperature ($^{\circ}\text{K}$), c_p is the specific heat of air at constant pressure ($1004 \text{ J } ^{\circ}\text{K kg}^{-1}$), ρ is the air density (kg m^{-3}), dp/dt is the pressure velocity denoted as ω (Pa s^{-1}), and dq/dt is the external diabatic heating rate ($\text{J m}^{-3} \text{ s}^{-1}$). Equation (1) is then vertically integrated over the depth of the entire troposphere, Z_o , to yield the equation (Bravar & Kavvas, 1991):

$$c_p M \frac{dT}{dt} = -\omega Z_o + \frac{dQ}{dt} \quad (2)$$

where T and ω indicate average values of temperature ($^{\circ}\text{K}$) and pressure velocity (Pa s^{-1}) respectively, while dQ/dt is the total external heating rate (W m^{-2}) in the troposphere. M is the mass of a vertical column between the ground surface and the pressure level of the tropopause ($20\,000 \text{ Pa}$) over a unit surface area of 1 m^2 . Mass M is expressed as the difference in pressures between the ground surface and the tropopause divided by the acceleration due to gravity (9.81 m s^{-2}). Equation (2) can be rewritten for an observer moving with the wave as:

$$c_p M \frac{DT}{Dt} = \frac{DQ}{Dt} \quad (3)$$

where $D/Dt = \partial/\partial t + c \cdot \partial/\partial x$ indicates the Lagrangian derivative in a frame of reference moving with the wave celerity c . Both the advective term and the adiabatic term ($-\omega Z_o$) are implicitly taken into account. DQ/Dt denotes the sink-source term of the thermodynamic energy equation.

The method of eigenfunction expansion (Haberman, 1987) is available in order to solve equation (3) numerically. Hence, the temperature field is expanded as a Fourier series:

$$T(x, t) = \sum_{i=1}^n T_i(t) \phi_i[x - x_i] \quad (4)$$

where $T_i(t)$, $i = 1, \dots, n$ are the Fourier components, $\phi_i[x - x_i] = \sin[(2\pi i)/L(x - x_i)]$ are basis functions composed of sine waves, $x_i = x_{0i} + c_i t$ are the phases of the temperature waves, L is the fundamental wave length, x_{0i} are origins of temperature waves, and c_i are celerities of temperature waves. Expressing the Lagrangian derivative D/Dt of temperature in terms of equation (4) yields:

$$\frac{DT}{Dt} = \sum_{i=1}^n \frac{dT_i}{dt} \phi_i + \sum_{i=1}^n T_i \left\{ \frac{\partial \phi_i}{\partial t} + c \frac{\partial \phi_i}{\partial x} \right\} \quad (5)$$

Since the wave celerity, c , is approximated to be c_i , the expression in brackets $\{\cdot\}$ is negligible (see Bravar & Kavvas, 1991, for details). Therefore, equation (5) may be approximated as:

$$\frac{DT}{Dt} = \sum_{i=1}^n \frac{dT_i}{dt} \phi_i \tag{6}$$

Equation (6) is substituted into equation (3) and the resulting equation is multiplied by one particular basis function ϕ_k . That result is then integrated over the Earth's circumference C_e . This manipulation amounts to projecting the equation which results from the combination of equations (3) and (6) onto the set of basis functions, ϕ_i . Due to the orthogonality of the basis functions a first order ordinary differential equation is obtained (Bravar & Kavvas, 1991):

$$c_p M \|\phi_i\| \frac{dT_i}{dt} = \int_0^{C_e} \frac{dQ}{dt} \phi_i [x - x_i] dx \quad i = 1, \dots, n \tag{7}$$

where $\|\phi_i\| = \int_0^{C_e} \{\phi_i [x - x_i]\}^2 dx$ is the norm of the i th basis function. In equation (7) the thermal sink-source term due to the shortwave radiation, longwave radiation, sensible heat flux and latent heat release is:

$$\frac{dQ}{dt} = S_r + L_r + H_g + L_c C \tag{8}$$

where S_r is the shortwave radiation absorbed in the troposphere ($W\ m^{-2}$), L_r is the longwave radiation absorbed in the troposphere ($W\ m^{-2}$), H_g is the sensible heat flux absorbed in the troposphere ($W\ m^{-2}$), L_c is the latent heat for condensation ($2.5 \times 10^6\ J\ kg^{-1}$), and C is the precipitation rate ($kg\ s^{-1}\ m^{-2}$).

In order to determine the celerities, c_i , of the temperature waves, the Rossby wave theory is applied by assuming a barotropic behaviour of the atmosphere (Rossby, 1939; Holton, 1992). The relationship between celerity, c_i , and wavelength, $L_i = i/L$, is given as:

$$c_i = U - \frac{L_i^2 \beta}{4\pi^2} \tag{9}$$

where U is the mean wind speed in the west-east direction. The average value of U in the troposphere at mid-latitude is assumed to be $7.5\ m\ s^{-1}$ (Palmen & Newton, 1969). The parameter β is the latitudinal change of the Coriolis factor. The value of β is assumed to be $3.0 \times 10^{-12}\ s^{-1}\ m^{-1}$ at mid-latitude. The celerities for each wave component are displayed in Table 1. The nonstationary Rossby wave components, which are characterized by the wavelengths from 3000 km to 10 000 km, are used in the model.

Table 1 Wave components used in the simplified model

K_i	3	4	5	6	7	8	9	10
L_i (km)	10 000	7500	6000	5000	4286	3750	3333	3000
c_i ($m\ s^{-1}$)	0.4	3.7	5.3	6.1	6.6	6.9	7.2	7.3
U_i ($m\ s^{-1}$)	5.6	4.2	3.3	2.8	2.4	2.1	1.9	1.7

K_i = wave number; L_i = wave length; c_i = celerity; U_i = advection speed of the i th W wave.

Atmospheric water balance

The balance of water vapour in the atmosphere is formulated as follows (Rasmussen, 1977):

$$\frac{dW}{dt} = \frac{\partial W}{\partial t} + V \cdot \nabla W = ET - C \quad (10)$$

where W is the total mass of water vapour in a vertical column of air with unit base (kg m^{-2}), $V \cdot \nabla W$ is the advection term of water vapour ($\text{kg m}^{-2} \text{s}^{-1}$), ET is the evaporation rate from soil or ocean surface ($\text{kg m}^{-2} \text{s}^{-1}$), and C is the precipitation rate ($\text{kg m}^{-2} \text{s}^{-1}$). Solving equation (10) numerically by using the same procedure which was adopted to deduce equation (7) yields (Bravar & Kavvas, 1991):

$$W(x, t) = \sum_{i=1}^n W_i(t) \phi[x - \xi_i] \quad (11)$$

$$\|\phi_i\| \frac{dW_i}{dt} = \int_0^{c_e} (ET - C) \phi_i[x - \xi_i] dx \quad i = 1, \dots, n \quad (12)$$

where W_i , $i = 1, \dots, n$ are the Fourier components, $\phi_i[x - \xi_i]$ are the basis functions as defined before, $\xi_i = \xi_{0i} + U_i t$ are phases of the waves at wind speeds U_i , and ξ_{0i} are the origins of the waves. The celerities of W waves are assumed to be equal to the average wind speeds. The shortwave components of W , which exist in the lower troposphere, have small wind velocity. This leads to the assumption that shorter water vapour waves move more slowly than those with longer wavelengths. The celerities of W waves, U_i , are also shown in Table 1.

Land and sea thermal balance

The thermal balance at the land (sea) surface is formulated as follows (Stull, 1988):

$$z_g c_g \frac{dT_g}{dt} = R_n - H_g - L \cdot ET \quad (13)$$

where z_g is the effective thickness of the soil (sea) layer (m), c_g is the thermal capacity ($\text{J m}^{-3} \text{ }^\circ\text{K}^{-1}$), T_g is the soil or sea temperature ($^\circ\text{K}$), and R_n is the net radiative flux at the land (sea) surface (W m^{-2}). It is assumed that the change of temperature beneath the soil (sea) layer is negligible and that the temperature profile in this soil (sea) layer is constant. The values of effective thickness, z_g , are assumed to be 0.5 m for soil and 70 m for the sea, while the values of thermal capacity, c_g , are $2.50 \times 10^5 \text{ J m}^{-3} \text{ }^\circ\text{K}^{-1}$ for soil (Corby *et al.*, 1977)

and $4.25 \times 10^6 \text{ J m}^{-3} \text{ }^\circ\text{K}^{-1}$ for the sea (Sellers & McGuffie, 1987). By modelling the thin layers of soil and sea, the net radiative flux at the ground is formulated as follows:

$$R_n = I_s + R_b - F_g \tag{14}$$

where I_s is the incoming shortwave radiation (W m^{-2}), R_b is the incoming longwave radiation emitted by the atmosphere (W m^{-2}), and F_g is the outgoing longwave radiation emitted by the land (sea) surface (W m^{-2}). Numerical solution for land (sea) surface temperature, T_g , is expressed by a Fourier series:

$$T_g(x, t) = \sum_{i=1}^m T_{gi}(t)\varphi_i(x) \tag{15}$$

$$z_g c_g \parallel \varphi_i \parallel \frac{dT_{gi}}{dt} = \int_0^l (R_n - H_g - L \cdot ET)\varphi_i(x)dx \quad i = 1, \dots, m \tag{16}$$

where T_{gi} , $i = 1, \dots, m$ are the Fourier components, $\varphi_i(x)$ are basis functions, and l is the effective length of a wave, taken as the longitudinal length of the continent or ocean.

Hydrological water balance

The water balance over the land area is modelled as follows (Thorntwaite & Matter, 1955):

$$\frac{dW_g}{dt} = -k \cdot W_g - ET + C \tag{17}$$

where W_g is the amount of water stored in the hydrological system and k is a constant coefficient ($1.4 \times 10^{-8} \text{ s}^{-1}$). The first term in the right hand side of equation (17) denotes water losses due to surface runoff, subsurface flow, and groundwater recharge. The value of k represents the inverse of time necessary to reduce the water storage to $1/e$ of its initial value if neither precipitation nor evaporation occur. Equation (17) is solved numerically by using the method of eigenfunction expansion yielding:

$$W_g(x, t) = \sum_{i=1}^m W_{gi}(t)\varphi_i(x) \tag{18}$$

$$\parallel \varphi_i \parallel \left[\frac{dW_{gi}}{dt} + k \cdot W_{gi} \right] = \int_0^l (-ET + C)\varphi_i(x)dx \quad i = 1, \dots, m \tag{19}$$

where W_{gi} , $i = 1, \dots, m$ are the Fourier components and $\varphi_i(x)$ are basis functions. The hydrological water balance is modelled only over the land area.

PARAMETERIZATION

This simplified climate model, in which the spatial resolution is of the order of 10^6 m, requires the subgrid scale parameterizations of heat and mass transports. The global thermal condition is dominated by the radiation balance as well as by the exchange of sensible heat flux in the atmosphere-ground system and the generation of latent heat flux due to precipitation or evaporation (Wallace & Hobbs, 1977). Equations (3) and (13) describe the global thermal balance. Water amount in the ground is supplied by precipitation and lost by evapotranspiration and *vice versa* for atmospheric water vapour. Equations (10) and (17) describe the global water balance. Sink-source terms in each basic equation described in the above section must be reasonably parameterized. The parameterizations used in the simplified climate model are described below. These parameterizations are significantly different from those used by Bravar & Kavvas (1991) in the earlier version of the climate model.

As a significant difference from the 1-layer climate model of Bravar & Kavvas (1991), in the simplified climate model the modelled atmosphere consists of two tropospheric layers and a stratospheric layer. The first layer (layer 1) extends from the surface pressure level to the 50 kPa (500 mb) pressure level, while the second layer (layer 2) extends from the 50 kPa pressure level to the 20 kPa (200 mb) pressure level which is defined as the tropopause (see Fig. 1). The stratosphere (layer 3) is in a thermal equilibrium state. The lapse rate of temperature is assumed to be constant, 0.0042 °K m^{-1} , in the troposphere. Relationships between temperature, pressure, and elevation are based on the hydrostatic and ideal gas equations (Wallace & Hobbs, 1977).

Longwave radiation

The atmospheric heat balance due to the longwave radiation is based on emission and absorption of heat at each layer (see Fig. 2). The formulations involved in the longwave radiation flux are based on Sellers (1973). The longwave radiation flux absorbed in the troposphere, L_r ($W m^{-2}$), is given by the following equation:

$$L_r = (1 - N) \left[\epsilon_T \epsilon_g \sigma T_g^A - (2 - \epsilon_2) F_1 - (2 - \epsilon_1) F_2 + \epsilon_T F_3 \right] + N \left[\epsilon_g \sigma T_g^A - (2 - \epsilon_1 - \epsilon_2) 0.5 \sigma (T_1^A + T_2^A) + F_3 \right] \quad (20)$$

where:

$$F_i = \epsilon_i \sigma T_i^A \quad i = 1, 2, 3 \quad (21)$$

and F_i is longwave radiation flux emitted by the i th layer due to the absorbing gas ($W m^{-2}$), ϵ_i is the emissivity of the i th layer, ϵ_T is the total emissivity of the layers 1 and 2, ϵ_g is the emissivity of the ground, T_i is the temperature of the i th layer (°K), T_g is the soil or sea temperature (°K), T is the average tempera-

ture in the troposphere ($^{\circ}\text{K}$), N is the percent cloudiness, and σ is the Stefan-Boltzman constant ($5.67 \times 10^{-8} \text{ W m}^{-2} \text{ }^{\circ}\text{K}^{-1}$). The net longwave radiation flux at the ground surface R_b (W m^{-2}), is expressed as:

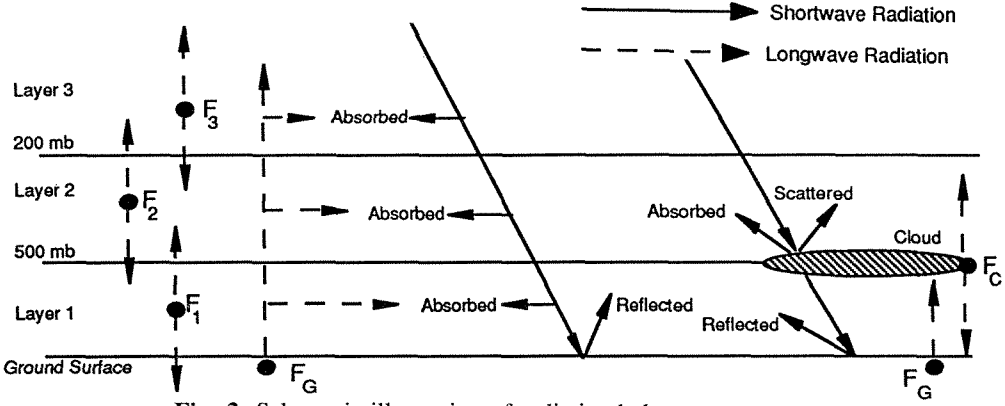


Fig. 2 Schematic illustration of radiation balance.

$$R_b = (1 - N) \left[-\epsilon_g \sigma T_g^A + F_1 + (1 - \epsilon_1) F_2 + (1 - \epsilon_T) F_3 \right] + N \left[(1 - \epsilon_2) 0.5 \sigma (T_1^A + T_2^A) \right] \quad (22)$$

in which the downward direction is positive. The upward longwave radiation flux at the tropopause, R_u (W m^{-2}) is expressed as:

$$R_u = (1 - N) \left[(1 - \epsilon_T) \epsilon_g \sigma T_g^A + (1 - \epsilon_2) F_1 + F_2 \right] + N \left[(1 - \epsilon_2) 0.5 \sigma (T_1^A + T_2^A) \right] \quad (23)$$

in which the upward direction is positive. The heat balance in the stratosphere is characterized by the thermal equilibrium state yielding:

$$S_3 + \epsilon_3 R_u - 2\epsilon_3 \sigma T_3^A = 0 \quad (24)$$

where S_3 is shortwave radiation absorbed in layer 3 (W m^{-2}), ϵ_3 is the emissivity of layer 3, and T_3 is the temperature of layer 3 ($^{\circ}\text{K}$).

Longwave radiation is absorbed by certain gases as well as by clouds in the atmosphere. Therefore, those amounts must be determined in order to quantify the heat balance. The absorbing gases included in the model are water vapour, carbon dioxide, and ozone.

The precipitable water vapour, u_w , which indicates water amount in a column, was empirically related to the surface vapour pressure by the following relationship (Sellers, 1973):

$$u_w = (0.123 + 0.152e_b) \frac{P_b}{P_0} \quad (25)$$

where u_ω is precipitable water vapour (g cm^{-2}), e_b is surface vapour pressure (mb), p_b is atmospheric pressure at the surface, and p_0 is standard pressure (10^5 Pa). The effective amount of water vapour involved in condensation, evaporation and precipitation processes exists only in the troposphere. Therefore, the precipitable water vapour in layer three, the stratosphere, is set to zero. Similar to the conceptualization of Sellers (1973), the precipitable water vapour at each layer, $u_{\omega i}$ (g cm^{-2}), in the troposphere is modelled as:

$$u_{\omega 2} = u_\omega \left[\frac{50\,000}{p_0} \right]^{1+6.22 \frac{e_b}{g \cdot u_\omega}} \quad (26a)$$

$$u_{\omega 1} = u_\omega - u_{\omega 2} \quad (26b)$$

The amount of carbon dioxide is determined by assuming a constant mixing ratio in the vertical column and is given as a function of pressure difference and concentration of CO_2 (Pielke, 1984):

$$u_{c1} = k_c \cdot C_c \cdot (p_b - 50\,000) \quad (27a)$$

$$u_{ci} = k_c \cdot C_c \cdot p_i \quad i = 2, 3 \quad (27b)$$

where u_{ci} is the actual amount of carbon dioxide at the i th layer (cm), k_c is a constant ($7.88 \times 10^{-6} \text{ cm Pa}^{-1}$ per ppm), p_i is the pressure at the i th layer (kPa), and C_c is the concentration of carbon dioxide (ppm).

Table 2 Effective pressure (Pa) of absorbing gases (after Sellers, 1973)

	H ₂ O	CO ₂
Layer 1	0.8 p_b	750
Layer 2	450	350
Layer 3		100

p_b = surface pressure (mb)

The pressure corrected optical path length ($u_{\omega i}^*$ for water vapour and u_{ci}^* for carbon dioxide at the i th layer) is used to determine the emissivity for each gas. This path length is assumed to be equal to the actual amount of gas multiplied by $(p_e/p_b)^\kappa$, where p_e is the effective gas pressure (Pa), and κ is a constant equal to 0.7 for water vapour and 0.67 for carbon dioxide. The p_e values for each gas are shown in Table 2. Emissivities for each gas are given by the following formulae (Sellers, 1973; Arakawa 1972):

$$\epsilon_{\omega i}(u_{\omega i}^*) = 1 - \frac{1}{1 + 1.75(u_{\omega i}^*)^{0.416}} \quad (28)$$

$$\epsilon_{ci}(u_{ci}^*) = 1 - (0.930 - 0.66 \log_{10} u_{ci}^*) \quad (29)$$

where ϵ_ω and ϵ_c are the emissivities of H_2O and CO_2 respectively. The effective amount of ozone is assumed to be all in the stratosphere. The fixed values of 0.3 cm for the optical path length, u_{o3}^* , and 0.030 for the emissivity, ϵ_{o3} , are used for layer 3. Total emissivities ϵ_i at each layer are given as the sum of the contributions from ozone, carbon dioxide and water.

In the model, a one-layer thin cloud is assumed to be located around the middle troposphere (see Fig. 2). The cloudiness is empirically determined as a function of the relative humidity at the ambient altitude (Washington & Williamson, 1977):

$$N = -0.6 + 1.15 \frac{\omega}{\omega_s} \quad (30)$$

where N is the percent cloudiness, ω is the mixing ratio of water vapour at the 75 kPa (750 mb) level (kg kg^{-1}), and ω_s is the saturation mixing ratio of water vapour at the 75 kPa level (kg kg^{-1}). The saturation mixing ratio can be formulated as a function of the ambient temperature as shown later.

Shortwave radiation

The shortwave radiation balance is shown schematically in Fig. 2. The spatial resolution of this simplified climate model exceeds one thousand kilometres and is unable to reproduce the diurnal cycle of the climate system. Therefore, in this study, the average daily insolation is used (Monin, 1986), ie:

$$S_0 = W_0 [(\sin\delta \sin\varphi)\psi + (\cos\delta \cos\varphi)\sin\psi] / \pi \quad (31a)$$

where

$$\psi = \cos^{-1}(\mp \tan\delta \tan\varphi) \quad (31b)$$

and W_0 is the solar constant (1380 W m^{-2}), φ is ambient latitude (rad), and δ is the declination angle of the sun (rad). The declination angle of the sun, δ , is assumed to be a fixed function of the day of the year:

$$\delta = \frac{23.45\pi}{180} \cos \left[\frac{2\pi D}{365} \right] \quad (32)$$

where D represents the number of days after 21 June.

Incoming shortwave radiation is divided into two parts by the wave length. One is the scattered part, S_0^s , which is subject to Rayleigh scattering and is 65.1% of S_0 . The other is the absorbed part, S_0^a , which is subject to atmospheric absorption and is 34.9% of S_0 (Arakawa, 1972).

The solar radiation is mainly absorbed by water vapour in the troposphere and by ozone in the stratosphere. The absorptivities due to water vapour and ozone for the absorbed part are defined respectively by the following equations (Arakawa 1972):

$$A_{\omega}(u_{\omega i}^* \sec \alpha) = 0.271(u_{\omega i}^* \sec \alpha)^{0.303} \quad (33a)$$

$$A_o(u_{oi}^* \sec \alpha) = 0.045(u_{oi}^* \sec \alpha + 8.34 \times 10^{-4})^{0.377} - 3.11 \times 10^{-3} \quad (33b)$$

where A_{ω} is the absorptivity of shortwave radiation due to water vapour, A_o is the absorptivity of shortwave radiation due to ozone, $u_{\omega i}^*$ is the effective path length of water vapour at the i th layer (g cm^{-2}), u_{oi}^* is the effective path length of ozone at the i th layer (cm), and α is the zenith angle of the sun (rad). In the case of a clear sky, the atmospheric albedo due to Rayleigh scattering is:

$$\alpha_0 = 0.085 - 0.245 \log_{10} \left[\frac{p_b}{p_0} \cos \alpha \right] \quad (34)$$

where α_0 is atmospheric albedo due to Rayleigh scattering. In the case of a clear sky, the shortwave radiation flux absorbed in the troposphere, S_r' (W m^{-2}), depends only on the optical path length of the absorbing gas, i.e.:

$$S_r' = S_0^a \left[1 - A_{\omega}(u_{\omega 3}^* \sec \alpha) - A_o(u_{o 3}^* \sec \alpha) \right] \left\{ A_{\omega} \left[\sum_{i=1}^3 u_{\omega i}^* \sec \alpha \right] - A_{\omega}(u_{\omega 3}^* \sec \alpha) \right\} \quad (35)$$

The shortwave radiation reaching the ground surface is reduced by scattering and absorption through the atmosphere, and by reflection from the albedo of the surface. Empirical values of surface albedo, α_s , are taken as 0.14 at the snow-free land surface and 0.07 at the ice-free sea surface. Then the shortwave radiation flux absorbed by the ground in the case of a clear sky, I_s' (W m^{-2}), is:

$$I_s' = (1 - \alpha_s) \left\{ S_0^a \left[1 - A_{\omega} \left[\sum_{i=1}^3 u_{\omega i}^* \sec \alpha \right] - A_o(u_{o 3}^* \sec \alpha) \right] + S_0^s \left[\frac{1 - \alpha_0}{1 - \alpha_0 \alpha_s} \right] \right\} \quad (36)$$

In the case of a cloudy sky, the absorbing gas and the cloud amount must be taken into account in order to determine the atmospheric optical path lengths. Assuming that the modelled cloud is located in the middle troposphere, as shown in Fig. 2, the equivalent optical path length of water vapour at the i th layer in the cloudy sky (g cm^{-2}), D_i is given by:

$$D_1 = (1 - N)u_{\omega 1}^* \sec \alpha + 1.66Nu_{\text{cloud}}^* \quad (37a)$$

$$D_i = u_{\omega i}^* \sec \alpha \quad i = 2, 3 \quad (37b)$$

where α is the zenith angle of the sun (rad), and u_{cloud}^* is the equivalent optical path length of the cloud (g cm^{-2}). The equivalent optical path length of the cloud depends on the type of cloud. A typical value of equivalent path length for a lower tropospheric cloud of 10 g cm^{-2} is used in the model. Absorbed

shortwave radiation is also reduced by the reflection due to the cloud. In order to account for this effect, the equivalent cloudiness for the absorbed part, N_a , is defined as the computed cloudiness N multiplied by the cloud albedo for the absorbed part, R_a (0.5 for the lower tropospheric cloud). The shortwave radiation flux absorbed in the troposphere in the case of a cloudy sky, S_r'' (W m^{-2}), is then expressed as:

$$S_r'' = S_0^a \left[1 - A_\omega(D_3) - A_o(u_{o3}^* \sec \alpha) \right] \left\{ A_\omega \left[\sum_{i=1}^3 D_i \right] - A_\omega(D_3) \right\} + S_0^a (1 - N_a) \left[A_\omega \left[\sum_{i=1}^3 D_i \right] - A_\omega \left[\sum_{i=2}^3 D_i \right] \right] \quad (38)$$

In order to estimate the shortwave radiation flux reaching the ground surface for a cloudy sky, the atmospheric albedo with cloud, α_c , is defined for the scattered part as follows:

$$\alpha_c = 1 - (1 - N_s)(1 - \alpha_o) \quad (39)$$

where N_s is the cloud amount for the scattered part, equal to the cloudiness N multiplied by the cloud albedo for the scattered part, R_s (taken as 0.66 for the lower tropospheric cloud considered here). The shortwave radiation absorbed by the ground in the case of a cloudy sky, I_s'' (W m^{-2}) is then expressed as:

$$I_s'' = (1 - \alpha_c) \times \left\{ \frac{S_0^a (1 - N_a)}{1 - \alpha_s N_s} \left[1 - A_\omega \left[\sum_{i=1}^3 D_i \right] - A_o(u_{o3}^* \sec \alpha) \right] + S_0^s \left[\frac{1 - \alpha_c}{1 - \alpha_c \alpha_s} \right] \right\} \quad (40)$$

The total amounts of the shortwave radiation absorbed in the troposphere and by the ground, S_r and I_s , respectively, are:

$$S_r = (1 - N)S_r' + NS_r'' \quad (41)$$

$$I_s = (1 - N)I_s' + NI_s'' \quad (42)$$

The shortwave radiation absorbed in the stratosphere, S_3 , is given as:

$$S_3 = S_0^a \left[A_\omega(u_{\omega 3}^* \sec \alpha) + A_o(u_{o3}^* \sec \alpha) \right] \quad (43)$$

Equation (43) is substituted into equation (24) to determine the downward flux from the stratosphere.

Sensible heat flux

The estimation of the sensible heat flux is based on the turbulent heat exchanges between the surface and the boundary layer defined above the

surface of the Earth (Washington & Williamson, 1977):

$$H_g = c_p \cdot C_d \cdot \rho_b \cdot |V_b| \cdot (T_g - T_b) \quad (44)$$

where H_g is the sensible heat flux from the ground surface (W m^{-2}), c_p is specific heat at constant pressure ($\text{J day}^{-1} \text{kg}^{-1}$), C_d is the drag coefficient (0.003), ρ_b is the air density at the bottom of the atmosphere (kg m^{-3}), and V_b is the surface wind speed (m s^{-1}). The surface wind speed is assumed to be 5 m s^{-1} in the model.

Evaporation

In order to evaluate a water balance over a watershed, the total evaporation from the free-water surface and the transpiration from the plants must be parameterized. Because the spatial resolution of the model is too large to take into account the distribution of plants, the evaporation rate in the model is used as an index of moisture flux at the surface instead of the evapotranspiration rate. The evaporation rate, ET , is formulated similarly to the sensible heat flux by considering the turbulent flux exchanges at the surface of the Earth. The potential evaporation rate, ET_p ($\text{kg m}^{-2} \text{s}^{-1}$) over the sea is given as (Churchill *et al.*, 1982):

$$ET_p = C_{d\omega} \cdot \rho_b \cdot |V_b| (\omega_{\omega_s} - \omega_b) \quad (45)$$

where $C_{d\omega}$ is a coefficient for evaporation ($C_{d\omega} = 0.7C_d$), ω_{ω_s} is the saturation mixing ratio of water vapour at the water surface subject to water temperature (kg kg^{-1}), and ω_b is the mixing ratio of water vapour in the surface boundary layer (kg kg^{-1}). The saturation mixing ratio of water vapour, ω_s , can be formulated as (Bosen, 1960; Wallace & Hobbs, 1977):

$$\omega_s = 0.622 \frac{e_s}{p} \quad (46)$$

where:

$$e_s = 33.8639[(0.00738T + 0.8072)^8 - 0.000019|1.8T + 48| + 0.0013] \quad (47)$$

where e_s is the saturation vapour pressure in mb, T is the ambient temperature ($^{\circ}\text{C}$), and p is the ambient pressure in mb. In order to use equation (45), the mixing ratio of water vapour in the surface boundary layer, ω_b , must be determined, i.e.:

$$\omega_b = \omega_{bs} \cdot RH \left[\frac{1 - 0.02}{p/p_b - 0.02} \right] \quad (48)$$

where ω_{bs} (mb) is the saturation mixing ratio in the surface boundary layer subject to the temperature at the bottom of the atmosphere and RH is the relative humidity at pressure level p . A distribution of relative humidity

provided by Manabe (1983) is assumed in order to determine the mixing ratio at any altitude.

Equation (45) is also used to determine the condensation rate of water vapour over water surfaces. For this purpose, ω_b (mb) is assumed to be 50% of ω . When the surface saturation mixing ratio (ω_{ω_s}) is larger than the mixing ratio in the surface boundary layer (ω_b), the evaporation takes place from the surface to the atmosphere. On the other hand, when ω_{ω_s} is less than the threshold value of ω_b , (0.5ω), condensation takes place from the atmosphere to the surface.

Since the potential evaporation rate given by equation (45) is valid only over the free-water surfaces, the actual evaporation rate over the land surfaces must still be provided. In order to take into account free convection, which effectively transports heat and moisture to the atmosphere, the evaporation coefficient in the case of land surfaces is 1.5 times larger than the value of the coefficient for free-water surfaces. The actual evaporation rate, ET ($\text{kg m}^{-2} \text{s}^{-1}$) is given as follows (Thorntwaite & Matter, 1955; Budyko, 1958):

$$ET = 1.5 \frac{W_g - W_{g\min}}{W_{g\max} - W_{g\min}} C_{d\omega} \rho_b \cdot |V_b| (\omega_{gs} - \omega_b) \tag{49}$$

where W_g is the amount of water stored in the hydrological system, $W_{g\max}$ is the maximum storage of water for which evaporation would achieve its potential value (kg m^{-2}), $W_{g\min}$ is the value of W_g at which evaporation is assumed to be negligible (kg m^{-2}) and ω_{gs} is the surface saturation mixing ratio subject to soil temperature (kg kg^{-1}). The condensation process over the land surface (dew formation) is not considered because dew rapidly evaporates in the morning.

Precipitation

Condensation takes place when the mixing ratio exceeds the saturation mixing ratio (supersaturation). Condensed water might change to precipitation through any cloud physics process. In order to evaluate the cloud physics, the relationship between the water vapour, cloud, snow, ice and precipitation must be parameterized. However, a much simpler approach is taken here where precipitation is formulated by considering the condensation mechanism and using the Clausius-Clapeyron equation:

$$C = \frac{\omega - \omega_s}{1 + L_c^2 \omega_s / C_p R_v T^2} \cdot \frac{m}{\Delta t} \tag{50}$$

where C is the precipitation rate ($\text{k m}^{-2} \text{s}^{-1}$), ω_s is the average saturation mixing ratio of water vapour in the troposphere (kg kg^{-1}), ω is the average mixing ratio of water vapour in the troposphere (kg kg^{-1}), R_v is the gas constant for moist air ($461 \text{ J kg}^{-1} \text{ }^\circ\text{K}^{-1}$), m is the fractional weight of the atmosphere (2000 kg m^{-2})

and Δt is the computational time interval (s). The precipitation rate, C , is defined only in the case of supersaturation. If the mixing ratio is less than the saturated mixing ratio, the precipitation rate is set to zero.

APPLICATION OF THE MODEL

The modified simplified climate model is applied for evaluation of the climate change only within the latitude band 30°N - 50°N . The mid-latitude of the northern hemisphere, in which the circumference, C_e , is about 30 000 km is considered as the computational domain. The longitudinal domain for computation consists of 30 grid points with the grid size Δx being 1000 km. The topography, which is averaged with respect to longitude and latitude within a grid interval, is incorporated into the model (Berkofsky & Bertoni, 1955). The relationships between the elevation, pressure and temperature are modelled so that the topographic effect on the thermal balance can be taken into account. The computational domain consists of Europe, Asia, the Pacific Ocean, North America and the Atlantic Ocean, as shown in Fig. 3. In order to estimate the diurnal change of the climate system and prevent computational divergence, the computational time step of Δt is fixed at 1 hour.

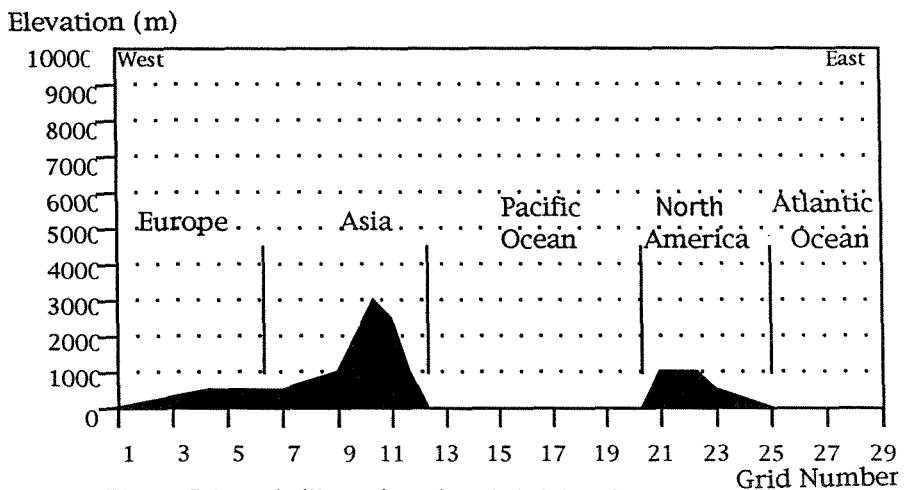


Fig. 3 Schematic illustration of modelled domain.

The first application of the model was to demonstrate that the model can reproduce values on the same order of magnitude as those of the average climate for the latitude band 30°N and 50°N . Fifty 25-year simulations were run each using slightly different initial amplitudes for the input variables. Ensemble averages were computed for each of the variables and the results are displayed in Table 3 where they are compared to values from Peixoto & Oort (1993). As can be seen from the results, the model is capable of reproducing the correct order of magnitude of the variables which determine climate.

Table 3 Modelled and observed mean climate values

Quantity	Model value	Observed value ¹
Surface air temperature (°C)	13	13
Soil temperature (°C)	12	-
Stratospheric temperature (°K)	224.5	223
Atmospheric moisture (g kg ⁻¹)	11	8
Land water storage (kg m ⁻²)	734	-
Evapotranspiration rate ² (m year ⁻¹)	0.3	0.35
Cloud cover (%)	47	55
Precipitation ² (m year ⁻¹)	0.48	0.5
Sensible heat flux (W m ⁻²)	32	29
Net radiation (W m ⁻²)	76.5	80

¹ from Peixoto & Oort (1993)

² averaged over land only

Since this model is to be used in the investigation of droughts in future studies, it must also be shown that the random changes in initial conditions do not induce drought-like effects. Figure 4 shows a plot of the ensemble average of the normalized water storage, W_g , over the 25 years of simulation corresponding to 50 realizations. It can be seen clearly that no particular trend exists once the model reaches the steady state and thus drought-like effects are not produced by random changes in the initial conditions.

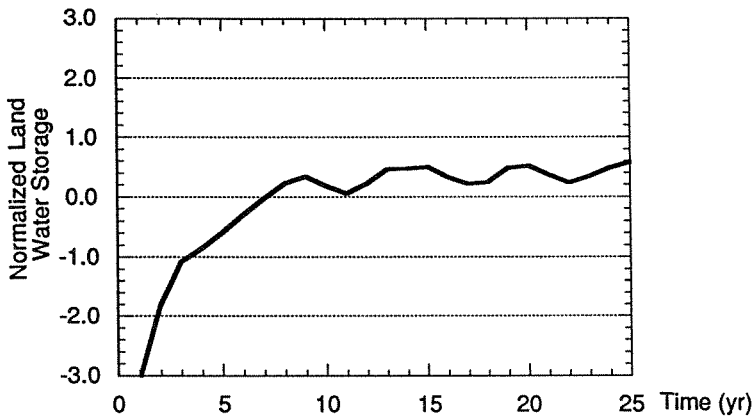


Fig. 4 Ensemble average of land water storage over time.

In the second set of simulations, an initial simulation for 100 years was performed in order to establish stable initial conditions. Then multiple runs were made for case studies in order to evaluate the effects of doubled carbon dioxide ($2 \times \text{CO}_2$) and quadrupled carbon dioxide ($4 \times \text{CO}_2$) on the climate. In the simulations, the computation was started at $t = 0$ years and the concentration of CO_2 held constant at 320 ppm ($1 \times \text{CO}_2$) for the first 20 years. Then, the CO_2 concentration was suddenly doubled or quadrupled on 1 January

at $t = 20$ years and the computation continued subsequently for three more decades. In the following Figures, the solid line indicates changes due to $2 \times \text{CO}_2$, while the dashed line indicates changes due to $4 \times \text{CO}_2$.

The change of annual mean heat flux absorbed in the whole troposphere, which corresponds to an annual mean value in the right-hand side of equation (1), is shown in Fig. 5. The results shown in Fig. 5 are consistent with previous investigations where the increase of heat flux absorbed in the atmosphere has been estimated to be 4 W m^{-2} when CO_2 is doubled. Thus, the change of heat balance in the atmosphere was properly reproduced.

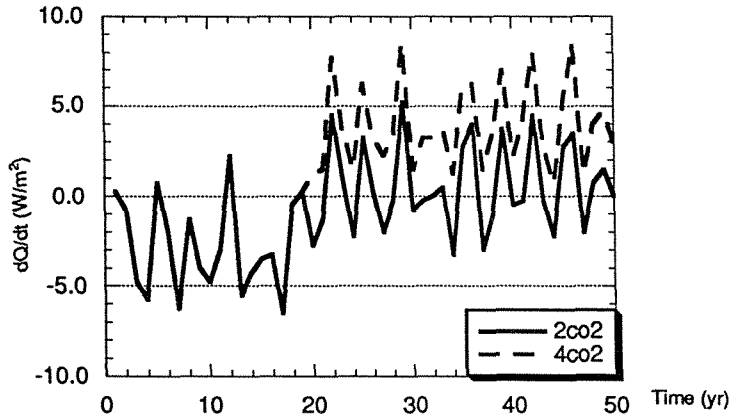


Fig. 5 Annual mean values for change of heat flux absorbed in the atmosphere over time for doubling and quadrupling CO_2 .

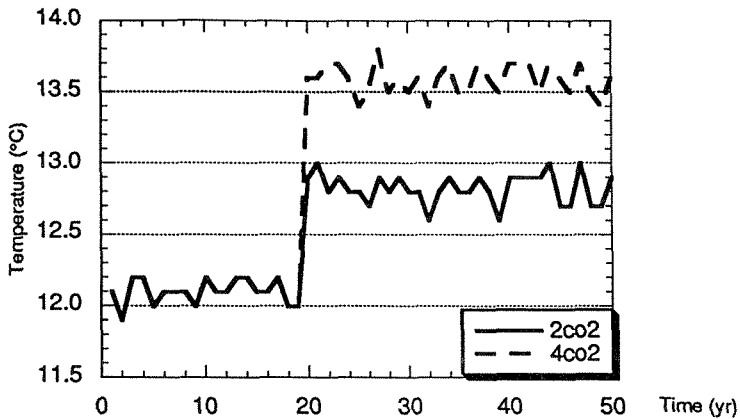


Fig. 6 Annual average atmospheric temperature at the Earth's surface over time with doubling and quadrupling of CO_2 .

The annual mean temperature at the ground averaged over all land areas changed with increase of CO_2 as shown in Fig. 6. Doubling of CO_2 caused a temperature increase of 1°C , while quadrupling causes a temperature increase of 1.5°C . Temperature changes due to doubling of CO_2 obtained by GCMs, which vary with the type of model and boundary conditions, are typically $2\text{--}3^\circ\text{C}$ as global mean values. Hence, the temperature changes calculated by

this model were rather small due in part to the simple cloud scheme and the constant albedo values used in the model. The pattern of soil temperature change was similar to that of atmospheric temperature.

Atmospheric water vapour amount increased due to increasing CO_2 as seen in Fig. 7. The water amount in the hydrological system, shown in Fig. 8 decreased initially at $t = 20$ years, but did not consistently remain lower. The change of annual mean evaporation rate averaged over all land areas is shown in Fig. 9, while that of precipitation rate is shown in Fig. 10. The results shown in Figs 9 and 10 indicate that although the precipitation rate decreased under climate change, it was still greater than the evapotranspiration rate after $t = 20$ years. The precipitation rate decrease can be explained by the increase in the value of the saturation vapour pressure with temperature. With the increase in atmospheric temperature comes an increase in the saturation vapour pressure. Because of the higher saturation vapour pressure, more water can evaporate into the atmosphere at or near the potential value which would mean the evaporative flux should not change much. The higher saturation vapour pressure also implies supersaturation conditions are harder to reach which would lead to a decreased precipitation rate. The pattern of decrease in the precipitation rate while the evapotranspiration rate remains almost the same after climate change could have an adverse effect on water storage, as seen in the case of $4 \times \text{CO}_2$ in Fig. 8. Further studies would have to be done to provide a more complete assessment of the decreased water storage shown in Fig. 8.

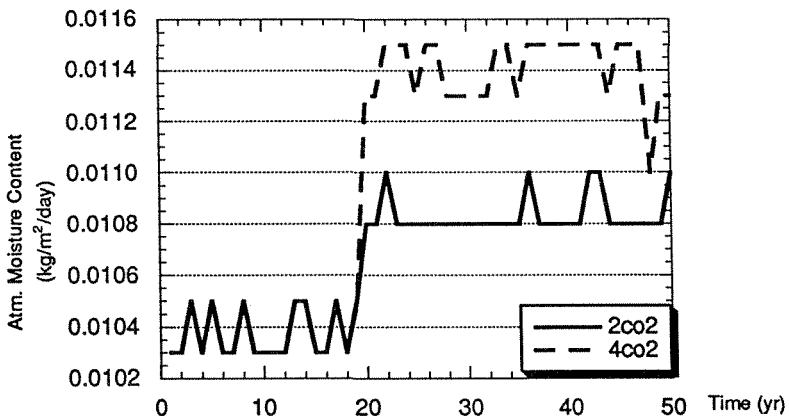


Fig. 7 Annual average atmospheric moisture content over time with doubling and quadrupling CO_2 .

The thermal equilibrium state, in which the absorbed radiation flux is identical to the emitted flux in a layer, is assumed for the calculation of stratospheric temperature. The stratospheric temperature change is shown in Fig. 11. According to the radiative convective (RC) models, which were proposed by Manabe and his co-workers, tropospheric temperature increases due to increasing CO_2 , while stratospheric temperature decreases (Manabe, 1983).

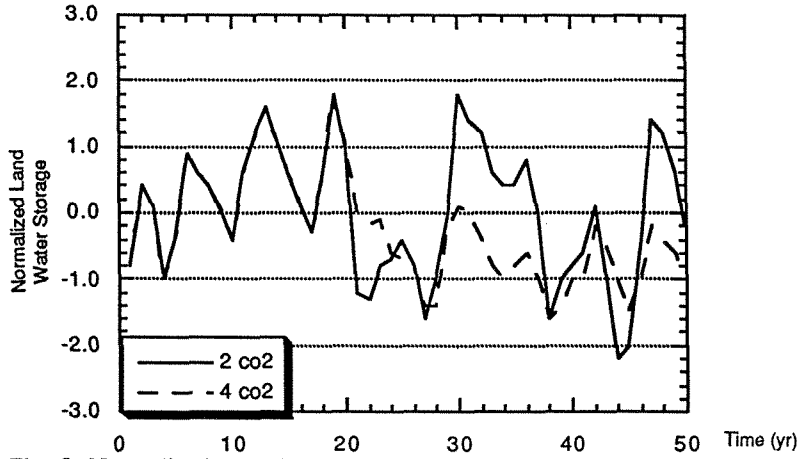


Fig. 8 Normalized annual average land water storage values over time for doubling and quadrupling of CO₂.

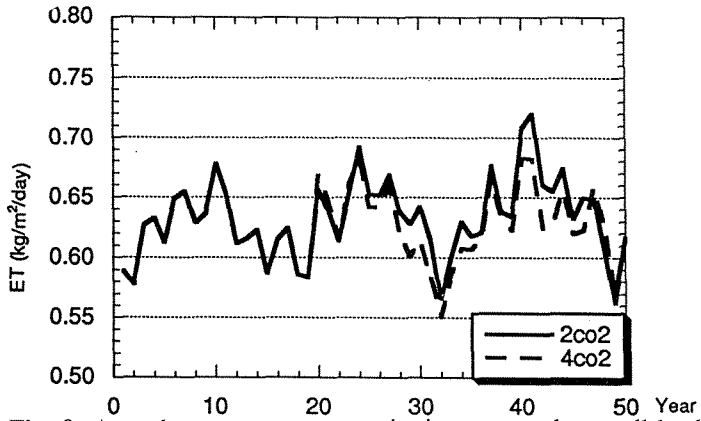


Fig. 9 Annual average evapotranspiration averaged over all land surfaces over time with doubling and quadrupling of CO₂.

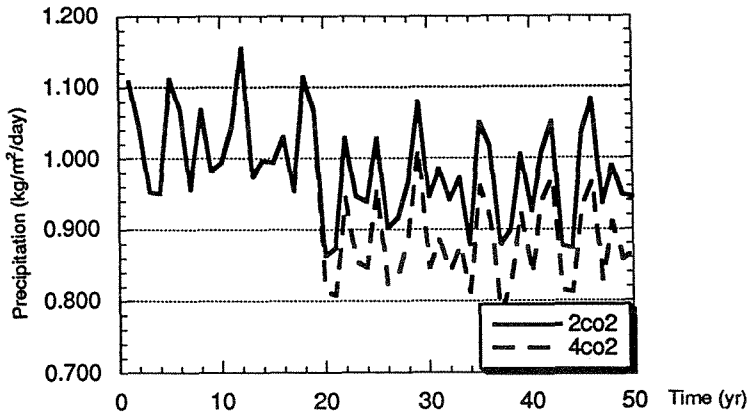


Fig. 10 Annual average precipitation averaged over all land surfaces over time with doubling and quadrupling of CO₂.

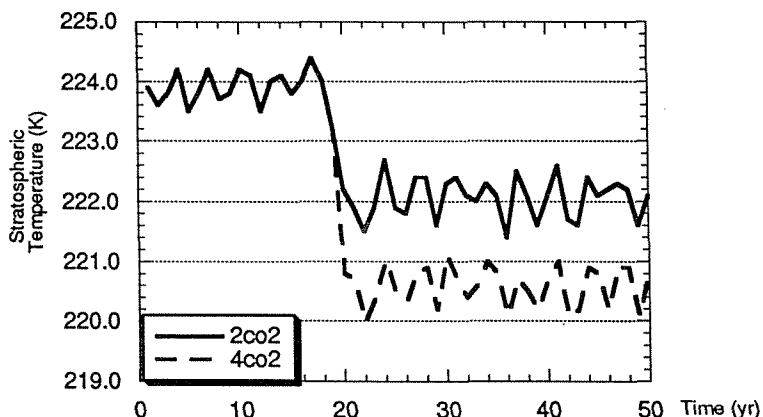


Fig. 11 Annual average stratospheric temperature over time for doubling and quadrupling CO_2 .

The simplified model presented here can reproduce a similar pattern of temperature as the RC models though the simulated result here is somewhat lower. Decreasing stratospheric temperature induces decreasing upward radiation flux at the upper atmosphere. Hence the outgoing radiation flux to space decreases so that the lower atmosphere, specifically the troposphere, warms up further.

Global warming is caused by not only the increase in CO_2 concentration but also by the increase of atmospheric water vapour content and the decreases of cloudiness and albedo. If the atmospheric temperature increases with an increase in CO_2 concentration, the increase in atmospheric water vapour content induces an additional increase in temperature. Such positive feedback effects that enhance the warming need to be modelled. For emissivity calculations, the relative humidity is kept constant in the model because it is assumed that the water vapour amount involved in the emissivity does not significantly change with time. However, by means of the radiation parameterizations which depend on water vapour, the increase of the atmospheric temperature is enhanced by an increase of the water vapour amount as a positive feedback effect. The physics-based parameterizations for cloudiness and change of albedo were not incorporated into the present model. In order to account for this positive feedback effect on temperature, these parameterizations shall be incorporated into the model in the near future.

CONCLUSION

In this study a simplified climate model, originally developed by Bravar & Kavvas (1991), was significantly modified with respect to its parameterizations. This model was then applied to simulations of climate change over the 30°N - 50°N latitude band around the Earth under $2 \times \text{CO}_2$ and $4 \times \text{CO}_2$ scenarios. Results of these simulations may be summarized as follows:

- (i) doubling the CO₂ concentration caused a 1°C increase in the annual mean temperature over the land surfaces while quadrupling the CO₂ concentration caused a 1.5°C increase;
- (ii) the warming mechanism (through positive feedbacks) due to the increase of atmospheric water vapour could be modelled adequately; and
- (iii) under CO₂ concentration increases, the evaporation rate tended to remain somewhat steady while the precipitation rate tended to decrease over the land surfaces.

These processes could lead to potential drought conditions. Improvements to the model parameterizations mentioned above will enable the model to reproduce better the physical processes associated with drought phenomena.

Acknowledgments The second and third authors gratefully acknowledge support by NSF Grant No. CMS-9318339. This work was also partially supported by the US EPA (R819658) Center for Ecological Health Research at UC Davis. This work does not necessarily reflect the views of the funding agency. L. Bravar of Università di Trieste had developed the original computer program for the earlier version of the climate model which was significantly modified and extended in this study. He has generously provided the authors with this original program version. The authors gratefully acknowledge this help and also thank him for discussions and insights on the topic.

REFERENCES

- Arakawa, A. (1972) Design of the UCLA general circulation model. Tech. Rep., 7, Dept. Met., UCLA, 91-116.
- Berkofsky, L. & Bertoni, E. A. (1955) Mean topographic charts for the entire earth. *Bull. Am. Meteor. Soc.* **36**, 350-354.
- Bosen, J. F. (1960) A formula for approximation of the saturation vapour pressure over water. *Mon. Weath. Rev.* August, 225-236.
- Bravar, L. & Kavvas, M. L. (1991) On the physics of droughts II. Analysis and simulation of the interaction of atmospheric and hydrological processes during droughts *J. Hydrol.* **129**, 299-330.
- Budyko, M. I. (1958) *Heat Balance at the Earth's Surface*. 1956, translated by N. A. Stepanova, US Weather Bureau, Washington DC, USA.
- Budyko, M. I. (1969) The effect of solar radiation variations on the climate of the Earth. *Tellus*, **21**, 611-619.
- Churchill, J. N., Ellyett, C. D. & Holmes, J. W. (1982) A study of regional evapotranspiration using remotely sensed and meteorological data – contrasts between forest and grassland. Australian Water Res. Council, Tech. Paper no. 70, Australian Gov. Pub. Serv., Canberra.
- Corby, G. A., Gilchrist, A. & Rowntree, P. R. (1977) United Kingdom Meteorological Office five-level general circulation model. In: *Methods in Computational Physics*. Academic Press, **17**, 67-110.
- Eagleson, P. S. (1970) *Dynamic Hydrology*, McGraw-Hill.
- Eagleson, P. S. (1978) Climate, soil, and vegetation. *Wat. Resour. Res.* **14**, 705-776.
- Haberman, R. (1987) *Elementary Applied Partial Differential Equations*. 2nd ed., Prentice-Hall.
- Hansen, J., Fung, I., Lacis, A., Rind, D., Lebedeff, S., Ruedy, R., Russell, G. & Stone, P. (1988) Global Climate Changes as Forecast by Goddard Institute for Space Studies Three Dimensional Model. *J. Geophys. Res.* **93**, 9341-9364.
- Holton, J. R. (1992) *An Introduction to Dynamic Meteorology*, Academic Press.
- Manabe, S. & Wetherald, R. T. (1967) Thermal equilibrium of the atmosphere with a given distribution of relative humidity. *J. Atmos. Sci.* **24**, 241-259.
- Manabe, S. & Bryan, K. (1969) Climate calculation with a combined ocean-atmospheric model. *J. Atmos. Sci.* **26**, 786-789.

- Manabe, S. (1983) Carbon dioxide and climate change. *Adv. Geophys.* **25**, 29-84.
- Meteorological Research Institute, Japan (1984) A description of the MRI atmospheric general circulation model. Tech. Rep. MRI, 13, Forecast Research Division, MRI, Japan.
- Monin, A. S. (1986) *An Introduction to the Theory of Climate*. D. Reidel Publishing Company, 10-13.
- Palmen, E. & Newton, C. W. (1969) *Atmospheric Circulation Systems*. Academic Press.
- Peixoto, J. & Oort, A. (1993) *Physics of Climate*. American Institute of Physics.
- Pielke, R. A. (1984) *Mesoscale Meteorological Modeling*. Academic Press, 191-200.
- Ramanathan, V. & Coakley, J. A. (1979) Climate modeling through radiative convective models. *Rev. Geophys. Space Phys.* **16**, 465-489.
- Rasmussen, E. M. (1977) Hydrological application of atmospheric vapour-flux analyses. Operational Hydrology Report. **11**, WMO, 476, WMO, Geneva, Switzerland.
- Rossby, C. G. (1939) Relation between variations in the intensity of the zonal circulation of the atmosphere and the displacement of the semi-permanent centers of action. *J. Mar. Res.* **2**, 38-55.
- Saltzman, B. (1978) A survey of statistical-dynamical models of the terrestrial climate. *Adv. Geophys.* **20**, 184-304.
- Sellers, A. H. & McGuffie, K. (1987) *Climate Modeling*. John Wiley & Sons.
- Sellers, W. D. (1965) *Physical Climatology*. The University of Chicago Press.
- Sellers, W. D. (1969) A global climatic model based on the energy balance of the Earth-atmosphere system. *J. Appl. Met.* **8**, 392-400.
- Sellers, W. D. (1973) A new global climatic model. *J. Appl. Met.* **12**, 241-254.
- Simmons, A. J. & Bengtsson, L. (1988) Atmospheric general circulation models: Their design and use for climate studies. In: *Physically Based Modelling and Simulation of Climate and Climatic Change - Part I*, ed M. E. Schlesinger, 23-76.
- Stull, R. B. (1988) *An Introduction to Boundary Layer Meteorology*. Kluwer, Dordrecht, The Netherlands.
- Thorntwaite, C. W. & Matter, J. R. (1955) *The water balance*. Publications in Climatology. **8** (1), Laboratory of Climatology, Centerton, NJ, USA.
- Wallace, J. M. & Hobbs, P. V. (1977) *Atmospheric Science, An Introductory Survey*. Academic Press.
- Washington, W. M. & Williamson, D. L. (1977) A description of the NCAR Global Circulation Models. In: *Methods in Computational Physics*. Academic Press, **17**, 111-173.

Received 6 November 1995; accepted 30 April 1996

LIST OF SYMBOLS

A_o	absorptivity of shortwave radiation due to ozone
A_w	absorptivity of shortwave radiation due to water vapour
C	precipitation rate
C_c	concentration of carbon dioxide
C_d	drag coefficient
C_e	circumference of the earth
C_{do}	evaporation coefficient
D	number of days after June 21
D_i	optical path length of water vapour at i-th layer for cloudy sky
ET	evaporation rate
ET_p	potential evaporation rate
F_i	longwave radiation emitted by the i-th layer
F_o	outgoing longwave radiation emitted by the surface
H_g	sensible heat flux
I_s	shortwave radiation absorbed at the ground surface
I_s^c	shortwave radiation absorbed at the ground surface for clear sky
I_s^c	shortwave radiation absorbed at the ground surface for cloudy sky
L	fundamental wave length
L_c	latent heat of condensation
L_i	wavelength of the i-th wave
L_r	longwave radiation absorbed in the troposphere
M	mass of a vertical column of unit surface area extending from the surface to the pressure level of the tropopause
N	percent cloudiness
N_s	cloud amount for scattered radiation
N_a	cloud amount for absorbed radiation
Q	total external heating
RH	relative humidity
R_b	incoming longwave radiation emitted by the atmosphere
R_n	net radiative flux at the land (sea) surface

R_u	upward longwave radiation flux at the tropopause
R_v	gas constant for moist air
S_3	shortwave radiation absorbed in stratosphere
S_0	average daily insolation
S_0^a	absorbed average daily insolation
S_0^s	scattered average daily insolation
S_r	shortwave radiation absorbed in the atmosphere
S_r'	shortwave radiation absorbed in the atmosphere for clear sky
S_r''	shortwave radiation absorbed in the atmosphere for cloudy sky
T	atmospheric temperature
T_b	temperature of the surface boundary layer
T_s	soil (sea) temperature
\bar{U}	mean wind speed in the east-west direction
V	wind velocity vector
V_b	surface wind speed
W	atmospheric water vapour mass in a vertical column of unit area
W	water stored in hydrological system
W_g^*	storage of water for which evaporation would achieve its potential value
W_g^{\max}	storage of water for which evaporation is assumed negligible
W_0	solar constant
Z_0	depth of the troposphere
c	wave celerity
c_g	thermal capacity
c_i	celerity of the i th wave
c_p	specific heat at constant pressure
e_b	surface vapour pressure
e_s	saturation vapour pressure
g	gravitational acceleration
k	inverse of time necessary for water storage to decrease to 1/e of its initial value
m	fractional weight of the atmosphere
p	pressure
p_b	atmospheric pressure at the surface
p_e	effective gas pressure
p_i	pressure of the i -th layer
p_0	standard pressure
q	external diabatic heating
t	time
u_{ci}	actual amount of carbon dioxide of the i th layer
u_ω	precipitable water vapour
$u_{\omega i}$	precipitable water vapour of the i th layer
$u_{\omega ci}$	pressure corrected optical path length for carbon dioxide
$u_{\omega o_3}$	pressure corrected optical path length for ozone
$u_{\omega w}$	pressure corrected optical path length for water vapour
$u_{c\text{cloud}}$	equivalent optical path length for cloud
z_g	effective thickness of soil (sea)
α	zenith angle
α_c	atmospheric albedo with cloud
α_s	surface albedo
α_0	atmospheric albedo due to Rayleigh scattering
β	latitudinal change of the Coriolis parameter
δ	declination angle of the sun
ϵ_g	emissivity of the ground
ϵ_i	emissivity of the i th layer
ϵ_T	total emissivity of layers 1 and 2
ϵ_{ci}	emissivity of carbon dioxide
ϵ_{o_3}	emissivity of ozone
$\epsilon_{\omega i}$	emissivity of water vapour
φ	latitude
ρ	density
ρ_b	air density at the surface
σ	Stefan-Boltzmann constant
ω	pressure velocity
ω_b	mixing ratio of water vapour in the surface boundary layer
ω_s	saturation mixing ratio of water vapour
ω_{bs}	saturation mixing ratio in the surface boundary layer subject to temperature of the surface boundary layer
ω_{gs}	surface saturation mixing ratio of water vapour subject to soil temperature
$\omega_{\omega s}$	saturation mixing ratio of water vapour at water surface subject to water temperature